Electronic Supplementary Material (ESI) for RSC Advances.

Supplementary Information

Combined *in silico* and *in vitro* study of aptasensor based on citrate-capped AuNPs for naked-eye detection of a critical biomarker of oxidative stress

Cherdpong Choodet,[a] Pakawat Toomjeen,[a] Witthawat Phanchai,[a] Piyaporn Matulakul,[a] Raynoo Thanan,[b,c,d] Chadamas Sakonsinsiri,[b,c,d] and Theerapong Puangmali[a,e,*]

[a] *Department of Physics, Faculty of Science, Khon Kaen University, Khon Kaen 40002, Thailand*

[b] *Department of Biochemistry, Faculty of Medicine, Khon Kaen University, Khon Kaen 40002, Thailand*

[c] *Cholangiocarcinoma Research Institute (CARI), Khon Kaen University, Khon Kaen 40002, Thailand*

[d] *Cholangiocarcinoma Screening and Care Program (CASCAP), Khon Kaen University, Khon Kaen 40002, Thailand*

[e] *Institute of Nanomaterials Research and Innovation for Energy (IN-RIE), Khon Kaen University, Khon Kaen, 40002, Thailand*

[*] *Corresponding author: E-mail: theerapong@kku.ac.th*

I. EXPERIMENTAL

A. Reagents

All oligonucleotides were synthesized by Integrated DNA Technologies (Integrated DNA Technologies, http://www.idtdna.com). All materials were used as received. Tetrachloroauric acid trihydrate ($HAuCl_4 \cdot 3H_2O$) was purchased from Merck Chemicals. Sodium citrate ($C_6H_5Na_3O_7 \cdot 2H_2O$) was purchased from Sigma-Aldrich.

B. Apparatus

The morphology of citrate-capped gold nanoparticles (AuNPs) was observed by transmission electron microscopy (TEM) (FEI 5022/22 Tecnai G2 20 S Twin, CR). UV-vis spectra were recorded by using Shimadzu, UV-1800. Dynamic light scattering (DLS) and zeta potential were measured by SZ-100 Horiba. The pH of the solution was measured by using Mettler Toledo LE438.

C. Synthesis of Citrated-Capped AuNPs

AuNPs were prepared by sodium citrate reduction method. Concisely, 2 mL of 0.1 M $HAuCl_4$ was mixed in a 198 ml deionized water. The solution was mixed by vigorous stirring. After boiling for 15 min, 20 mL of 38.8 mM sodium citrate was rapidly added into the solution. The resulting wine-red solution was filtered by a 0.45 μm filter paper and stored in the refrigerator (4°C) until use. The as-prepared AuNPs were characterized by using UV-vis spectroscopy, transmission electron microscopy (TEM), and dynamic light scattering (DLS). Based upon TEM micrographs, the average diameter of the AuNPs was 15 nm and the concentration of the AuNPs solution was 12 nM.

II. SUPPLEMENTARY INFORMATION

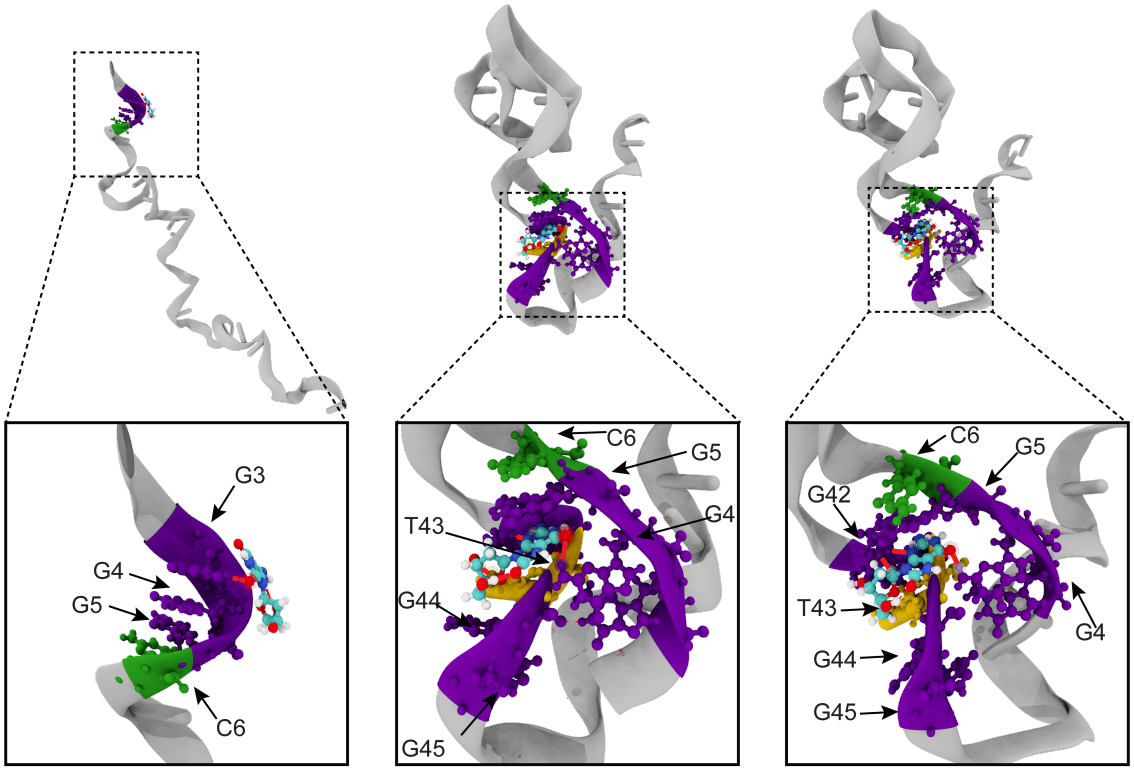

Fig. S1: Snapshots of the binding mechanism for 8-oxo-dG and its binding aptamer once 8-oxo-dG was placed at the top position of the aptamer. (a) Adsorption stage: 8-oxo-dG anchored to the binding sites G3, G4, G5, and C6. (b) Binding stage: 8-oxo-dG fitted into the recognition site of the aptamer by hydrogen bond formation with G4, G5, C6, T43, G44, and G45. (c) Complex stabilization stage: the hydrogen bonding interactions cooperatively stabilized the complex structure.

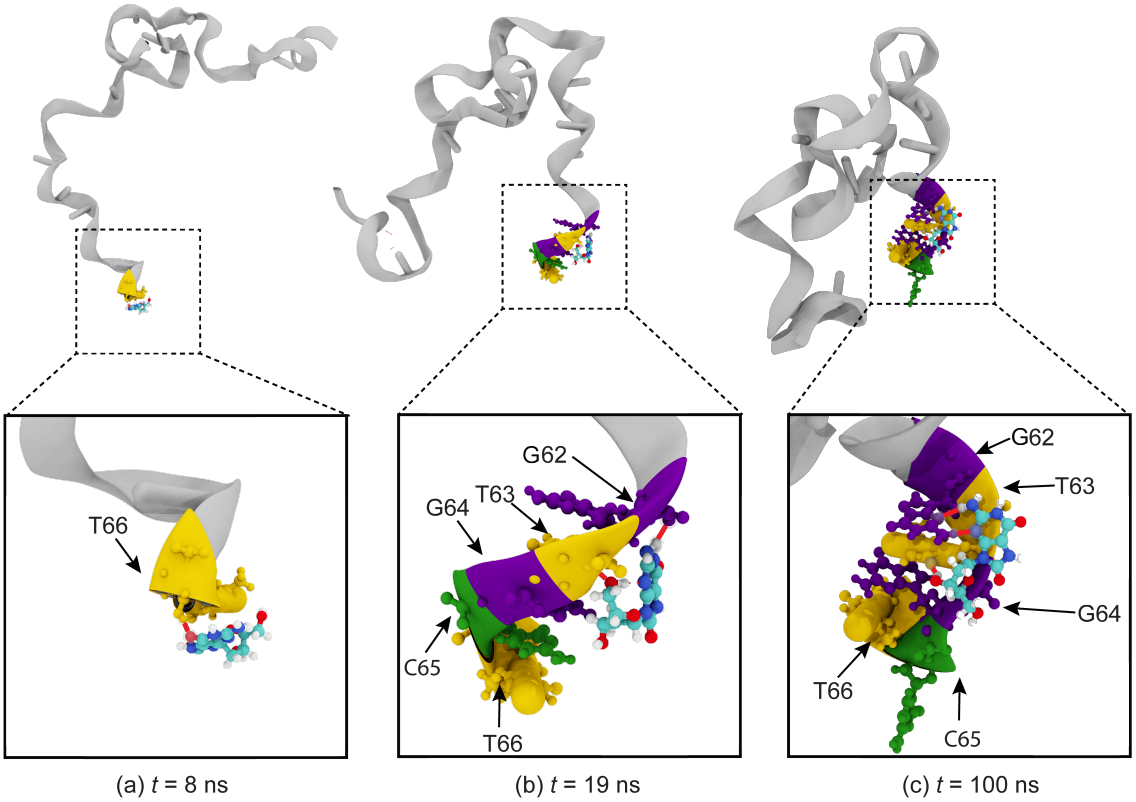

Fig. S2: Snapshots of the binding mechanism for 8-oxo-dG and its binding aptamer once 8-oxo-dG was placed at the bottom position of the aptamer. (a) Adsorption stage: 8-oxo-dG anchored to the binding site (T66). (b) Binding stage: 8-oxo-dG fitted into the recognition site of the aptamer by hydrogen bond formation with G62, T63, G64, C65, and T66. (c) Complex stabilization stage: the hydrogen bonding interactions cooperatively stabilized the complex structure.

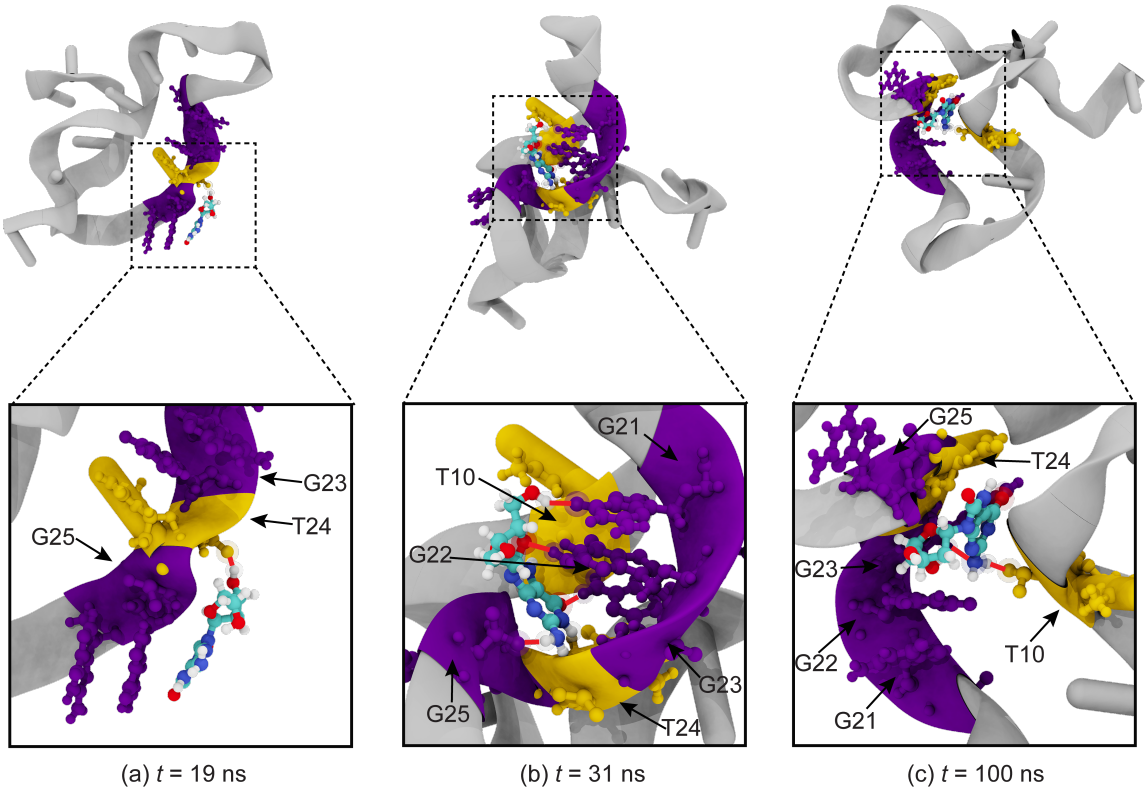

Fig. S3: Snapshots of the recognition interactions between 38-mer aptamer and 8-oxo-dG placed at the top position. (a) Adsorption stage: 8-oxo-dG anchored to the binding site (T24). (b) Binding stage: 8-oxo-dG fitted into the recognition site of aptamer by hydrogen bond formation with T10, G21, G22, G23, T24, and G25. (c) Complex stabilization stage: the hydrogen bonding interactions cooperatively stabilized the complex structure.

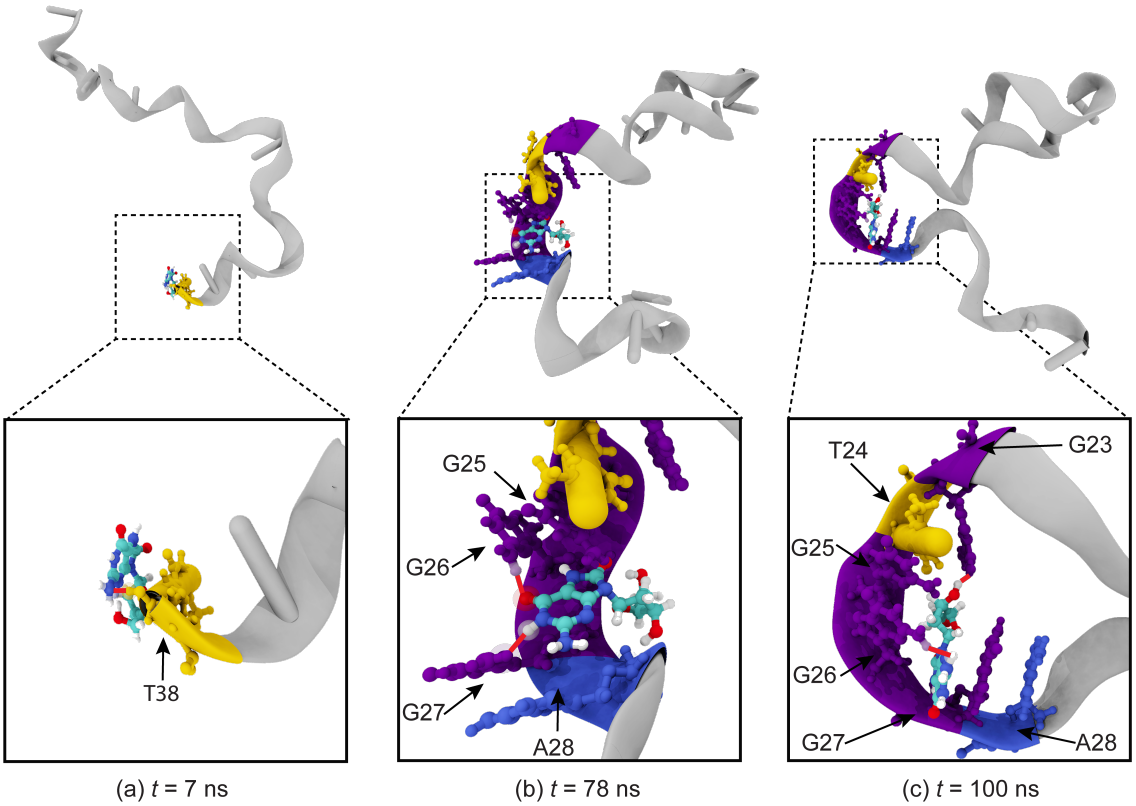

Fig. S4: Snapshots of the recognition interactions between 38-mer aptamer and 8-oxo-dG placed at the central position. (a) Adsorption stage: 8-oxo-dG anchored to the binding site (T38). (b) Binding stage: 8-oxo-dG fitted into the recognition site of the aptamer by hydrogen bond formation with G23, T24, G25, G26, G27, and A28. (c) Complex stabilization stage: the hydrogen bonding interactions cooperatively stabilized the complex structure.

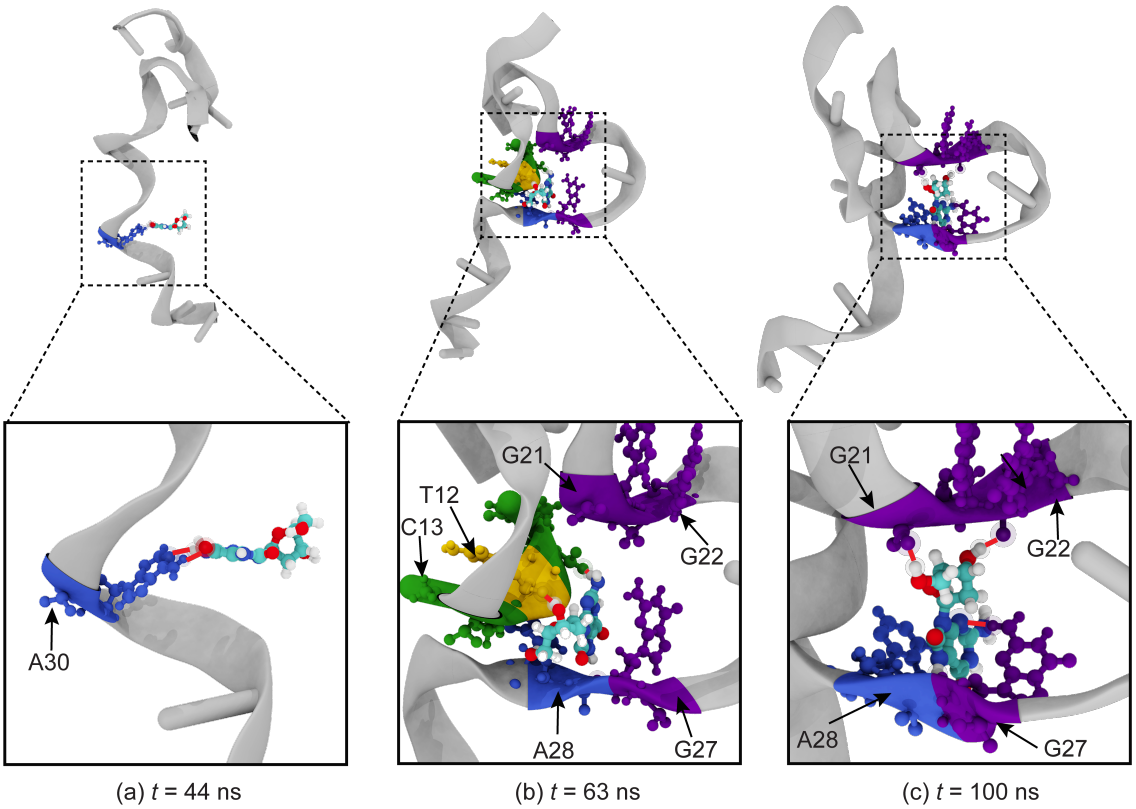

Fig. S5: Snapshots of the recognition interactions between 38-mer aptamer and 8-oxo-dG placed at the bottom position. (a) Adsorption stage: 8-oxo-dG anchored to the binding site (A30). (b) Binding stage: 8-oxo-dG fitted into the recognition site of the aptamer by hydrogen bond formation with T12, C13, G21, G22, G27, and A28. (c) Complex stabilization stage: the hydrogen bonding interactions cooperatively stabilized the complex structure.

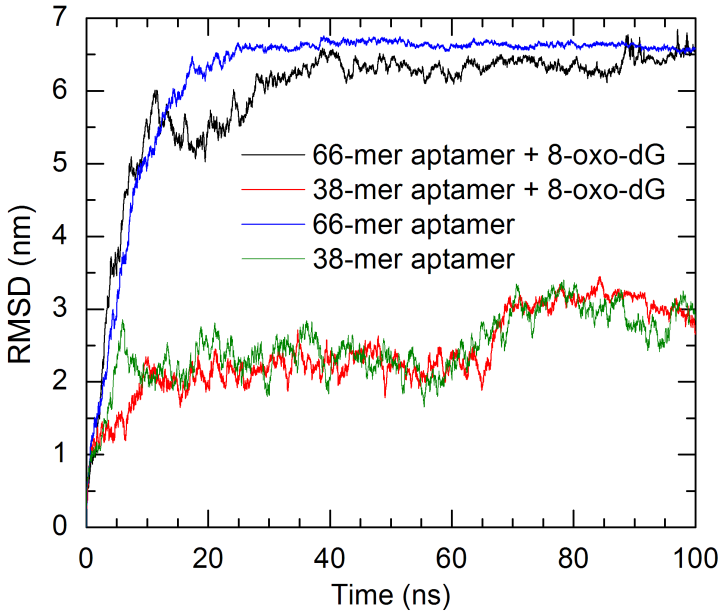

Fig. S6: RMSD plots of the conformational change of 66-mer and 38-mer aptamers in the presence and absence of 8-oxo-dG.

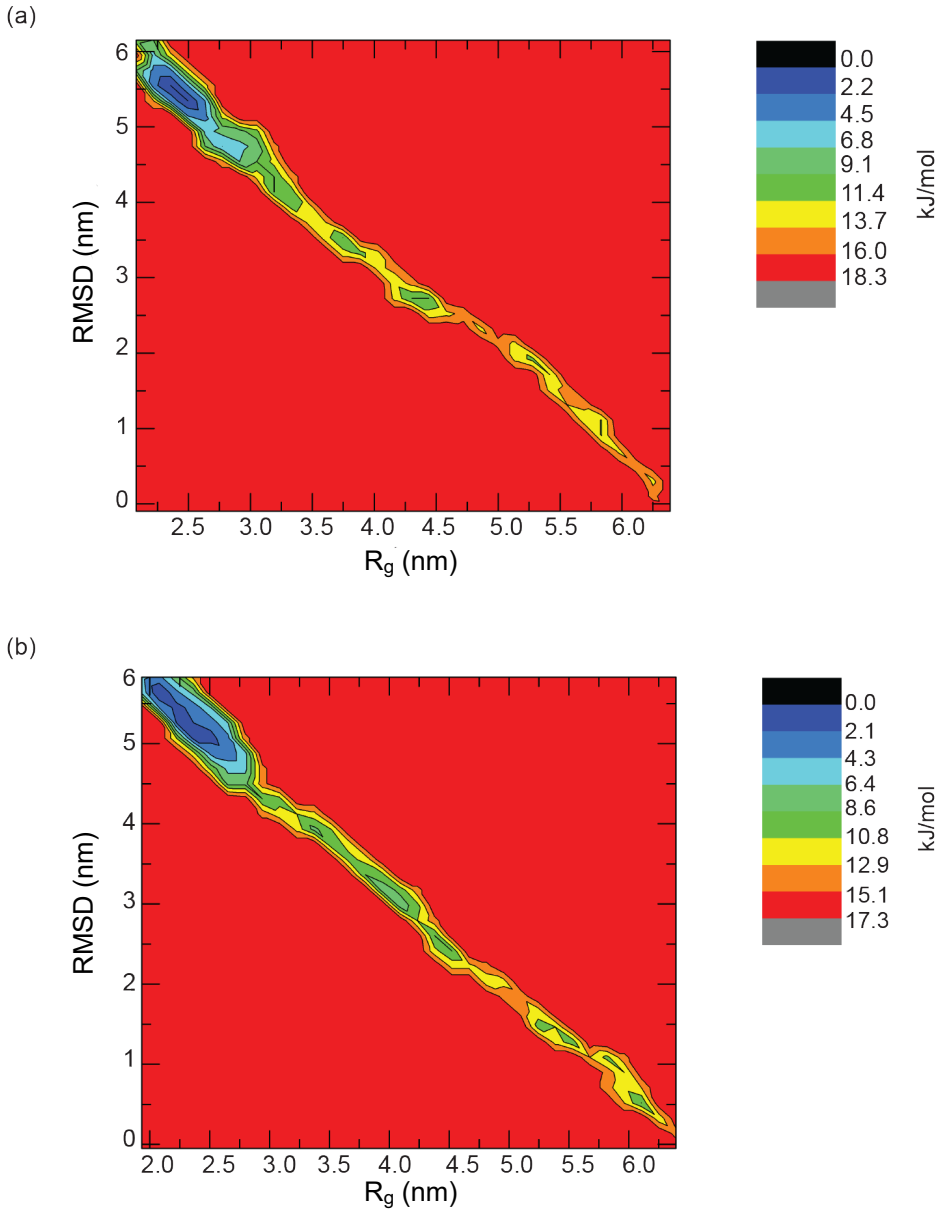

Fig. S7: The projected free energy contour plot between radius of gyration (R_g) and the root mean square deviation (RMSD) of 66-mer aptamer when the initial position of 8-oxo-dG was (a) at the top and (b) at the bottom of the aptamer. Different colours in the free energy landscapes represent different energy levels varying from blue (low energy) to red (high energy).

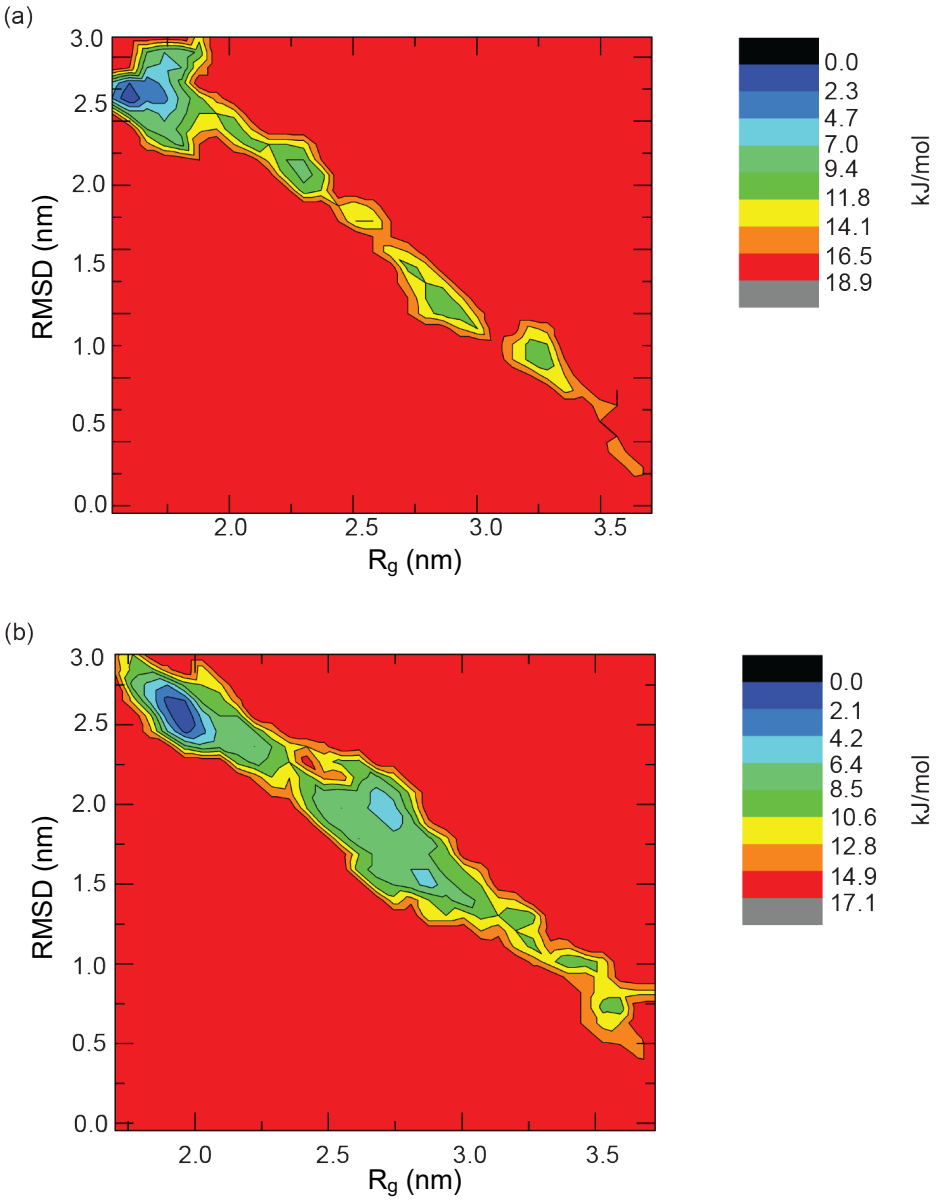

Fig. S8: The projected free energy contour plot between radius of gyration (R_g) and the root mean square deviation (RMSD) of 38-mer aptamer when the initial position of 8-oxo-dG was (a) at the top and (b) at the bottom of the aptamer. Different colours in the free energy landscapes represent different energy levels varying from blue (low energy) to red (high energy).

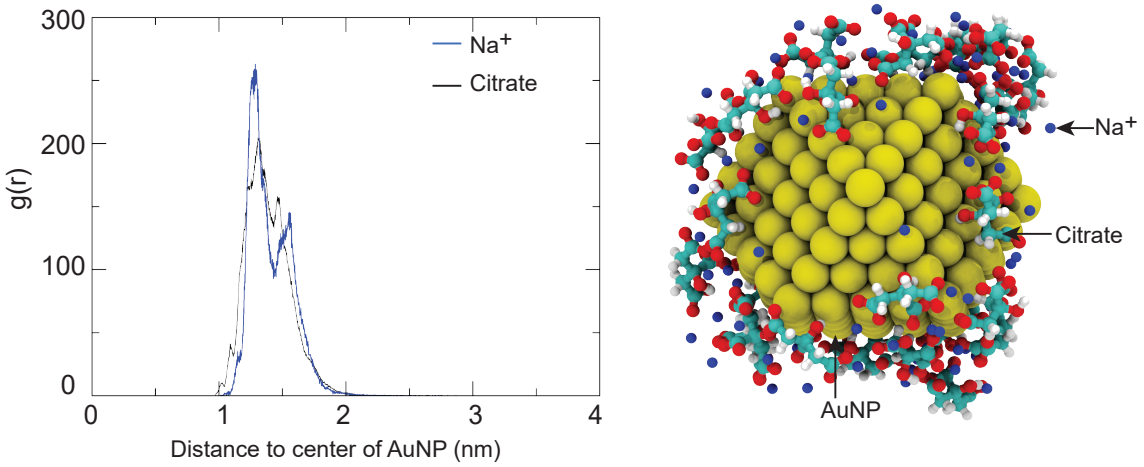

Fig. S9: Radial distribution function g(r) of 30 citrate molecules and Na ions (deep blue) around a 2-nm-in-diameter AuNP. Solvent is not shown for clarity.

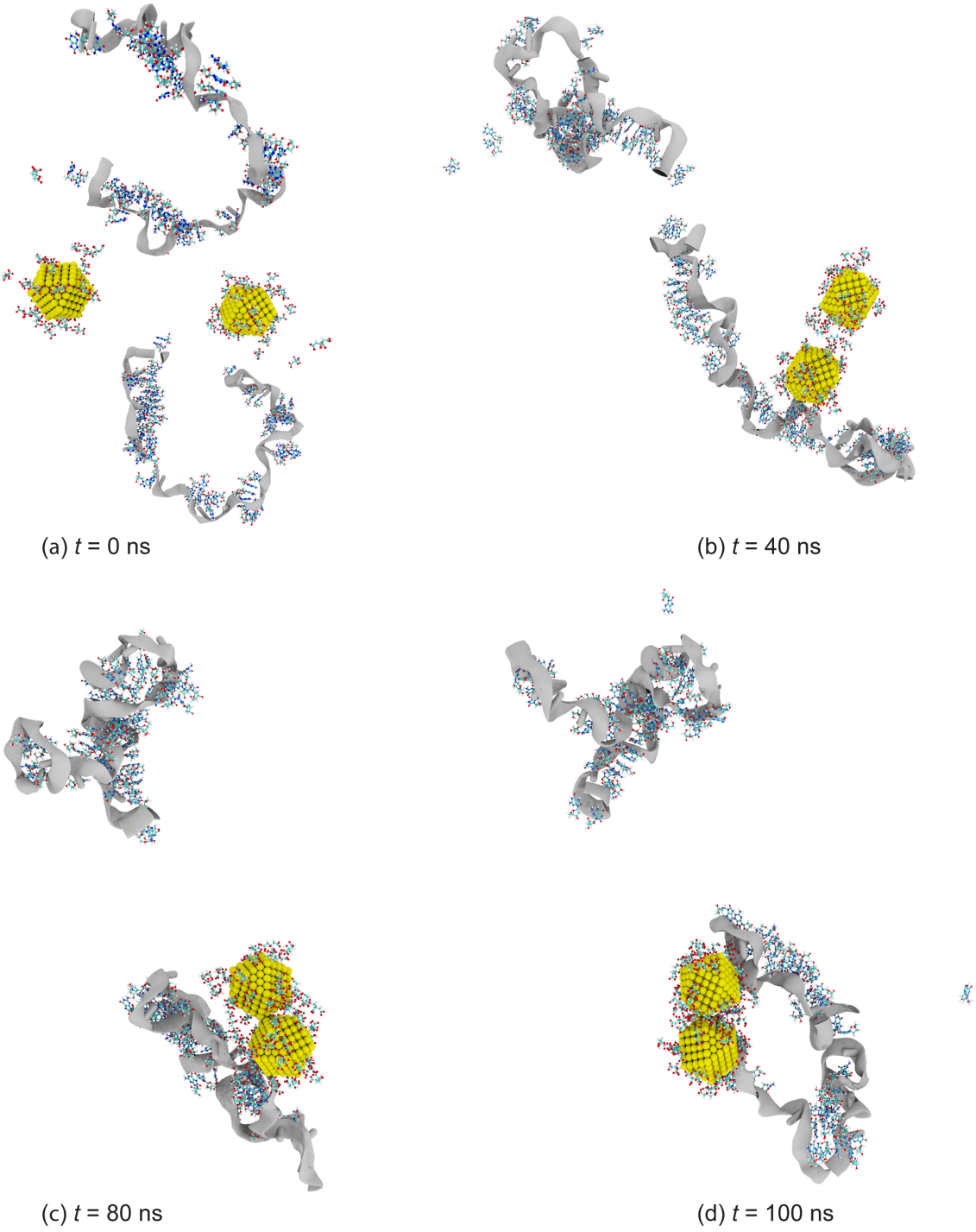

Fig. S10: Simulation snapshots of assembly of citrated-capped AuNPs in the presence of the aptamers bound with 8-oxo-dG molecules. The concentration of NaCl is 0.15 M. Due to the binding of 8-oxo-dG molecules with the aptamers, they no longer prevent AuNPs from aggregation under high salt concentration.

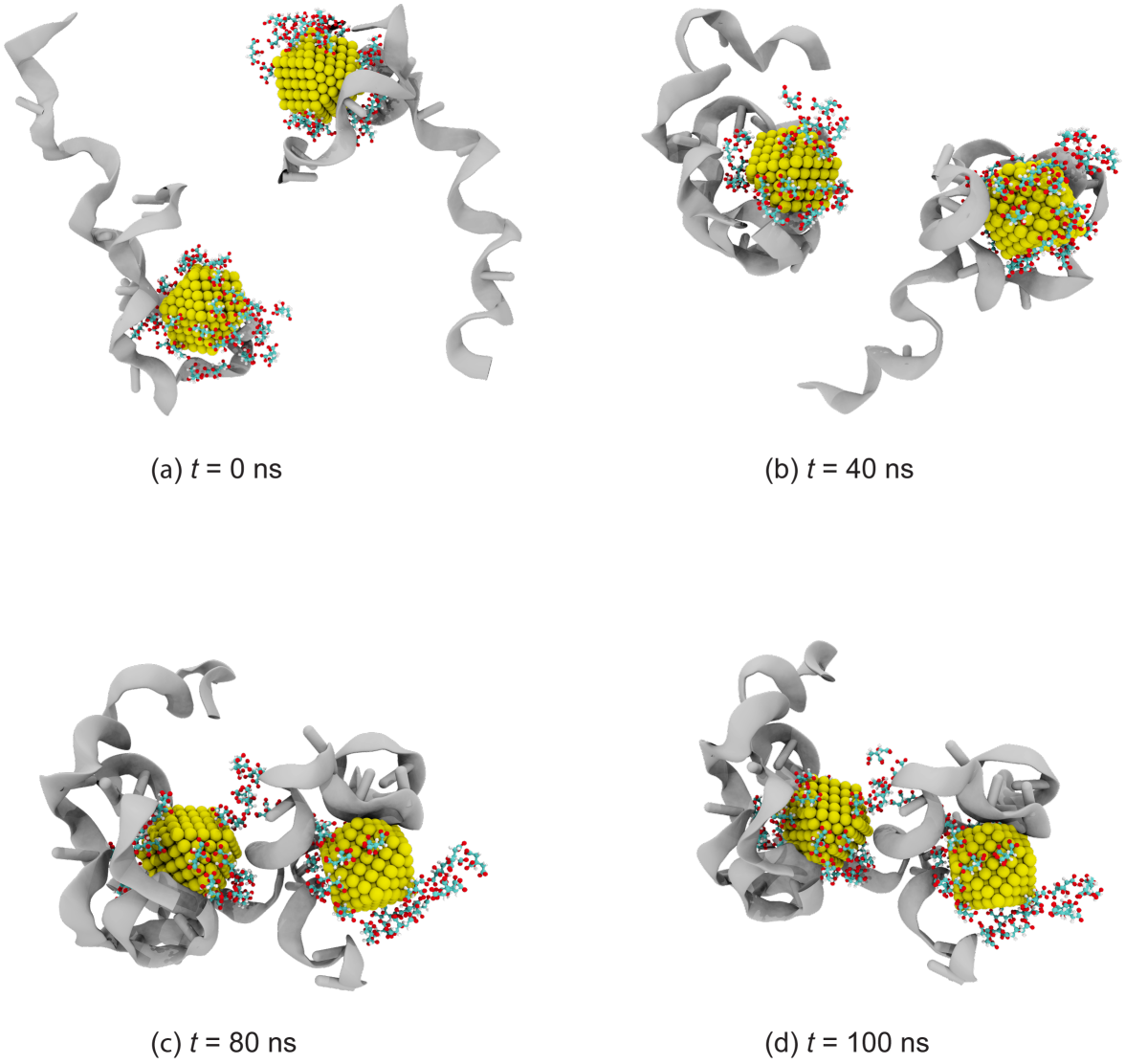

Fig. S11: Simulation snapshots of the interactions between two aptamer-bound AuNPs in the NaCl solution. The concentration of NaCl is 0.15 M. Solvent is not shown for clarity. The aptamers are shown in light grey. The adsorption of the aptamers onto the AuNP surfaces can prevent AuNPs from aggregation under high salt concentration.